JOURNAL OF AGRICULTURAL AND FOOD CHEMISTRY
ARTICLE

J. Agric. Food Chem. 2010, 58, 3667–3673 3667
DOI:10.1021/jf9042908

# Characterization of β-Lactoglobulin Fibrillar Assembly Using Atomic Force Microscopy, Polyacrylamide Gel Electrophoresis, and *in Situ* Fourier Transform Infrared Spectroscopy

Daniela Oboroceanu,[†,‡] Lizhe Wang,[†] André Brodkorb,[†] Edmond Magner,[‡] and Mark A. E. Auty*,[†]

[†]Moorepark Food Research Centre, Teagasc, Moorepark, Fermoy, County Cork, Ireland, and [‡]Materials and Surface Science Institute and Department of Chemical and Environmental Sciences, University of Limerick, Limerick, Ireland

The aggregation process of β-lactoglobulin (β-lg) from 0 min to 20 h was studied using atomic force microscopy (AFM), scanning transmission electron microscopy (STEM), sodium dodecyl sulfate−polyacrylamide gel electrophoresis (SDS−PAGE), and *in situ* attenuated total reflectance−Fourier transform infrared spectroscopy (ATR−FTIR). Fibril assembly was monitored in real time using AFM up to 20 h. From 0 to 85 min, β-lg monomers deformed and expanded with some aggregation. After 85 min, fibrillar structures were formed, exceeding 10 μm in length. Fibrillar structures were confirmed by STEM. Secondary structural changes occurring during fibril formation were monitored by ATR−FTIR at 80 °C and indicated a decrease in α-helix content and an increase in β-sheet content. SDS−PAGE indicated that fibrils were composed of polypeptides and not intact monomers. In this study, β-lg and whey protein isolate (WPI)-derived fibrils, including some double helices, in water were observed by AFM under ambient conditions and in their native aqueous environment.

**KEYWORDS: β-Lactoglobulin; whey protein isolate; proteins; peptides; self-assembly; fibrils; AFM; ATR−FTIR; SDS−PAGE; STEM**

## INTRODUCTION

Whey protein isolate (WPI) is extensively used as a functional ingredient in the food industry. Whey proteins in bovine milk contain a mixture of β-lactoglobulin (β-lg), α-lactalbumin, and bovine serum albumin, all of which may form fibrillar aggregates under specific conditions (*1*, *2*). β-lg is the major whey protein in cow's milk, representing ∼50% of the total whey protein content. β-lg is a globular milk protein, whose secondary structure contains approximately 50% β-sheet, 9−12% α-helix, 8−10% turn, and 30−35% random coil (*3*) and forms fibrillar aggregates 2−4 nm in thickness upon prolonged heating at low pH and low ionic strength (*4*, *5*). No fibrils are formed upon heating pure α-lactalbumin or bovine serum albumin at pH 2, but fibrils are formed in pure β-lg and WPI solutions (*1*, *2*, *6*, *7*). Various studies have shown that β-lg structures have the potential to be used as functional ingredients in food product foods because of their unique functional properties, for example, emulsification, gelation, thickening, foaming, and water-binding capacity (*8*−*10*). These protein fibrils could be used as thickening ingredients in low-calorie products, for example, as replacements for polysaccharide-based ingredients or meat replacement products and high protein content foods. The addition of small amounts of protein fibrils may increase the viscosity and shear thinning behavior of food products. Arnaudov et al. (*11*) established the critical concentration for fibril formation as 2.5 g $L^{-1}$ using nuclear magnetic resonance (NMR) spectroscopy and static light scattering, while atomic force microscopy (AFM) data suggested that the fibrils had an irregular helical structure, with a thickness of one or two protein monomers and a periodicity of approximately 28 nm. From the literature (*4*, *6*, *11*, *12*), the effect of increasing the ionic strength using NaCl or $CaCl_2$ on the morphology of the fibrilar aggregates formed from β-lg at pH 2.0 upon heating at 80 °C leads to an increase of the rate of fibril formation but a decrease in length, most likely because of screening of electrostatic repulsion. At low ionic strength, the β-lg fibrils are long and straight, whereas at high ionic strength (≥0.08), they are short and curved. The fibrils obtained at all ionic strengths exhibit similar thicknesses and periodic morphology. Similar results showed that fine-stranded aggregates of β-lg appeared as strings of monomers (*13*). Nevertheless, a more recent study suggests that β-lg fibrils formed at pH 2 were composed of peptides and that intact β-lg was not present in the fibrils (*14*). In biopolymer studies, AFM has become a standard investigation technique for visualizing the structures at the molecular scale (*15*−*17*). In this study, oscillatory or "AC" mode was used to investigate the fibrillar assembly process of β-lg heated at 80 °C. During AFM investigations, biological samples can be damaged or dragged across the substrate because of the mechanical contact with the tip. To avoid this, good sample−substrate binding and a small

*To whom correspondence should be addressed. Telephone: +353-25-42442. Fax: +353-25-42340. E-mail: mark.auty@teagasc.ie.


Published on Web 02/26/2010

sample−tip contact area are required. Using AC (otherwise known as "tapping" or "oscillatory") mode prevents sample damage and avoids the trapping of the AFM tip by capillary forces between the tip and the sample. A difficulty with previously reported AFM data is that images were obtained in an ambient air environment, which could affect the appearance of the fibrils (*18*). To overcome this drawback, AFM imaging of $\beta$-lg and WPI in liquid and air environments was performed and the results were compared. It has been argued that electrostatic or hydrophobic interactions with the mica surface affect the morphology and elongation pattern of the fibrils as determined by AFM (*19*). Therefore, to confirm that fibrillar structures were formed, scanning transmission electron microscopy (STEM) was also performed on selected samples in this study. Previous research showed that $\beta$-sheet content presents a spectral band at ~1630 $cm^{-1}$, while α-helix content presents a spectral band at 1654 $cm^{-1}$ (*20*, *21*). To clarify the process of fibril formation in a $\beta$-lg dispersion heated at 80 °C and pH 2, we followed changes in secondary protein structure in real time using attenuated total reflectance−Fourier transform infrared spectroscopy (ATR−FTIR) at 80 °C. Sodium dodecyl sulfate−polyacrylamide gel electrophoresis (SDS−PAGE) analyses under reducing conditions were also performed to investigate time-dependent changes in the molecular weights of $\beta$-lg fractions, specifically to determine whether fibrils were composed of $\beta$-lg monomers or polypeptide fragments. The fibril formation processes of $\beta$-lg and WPI are similar. For investigation methods requiring large amounts of fibril dispersion, WPI is a standard ingredient used by the food industry. $\beta$-lg (Sigma grade) was used for SDS−PAGE analysis.

## MATERIALS AND METHODS

**Sample Preparation.** Bovine $\beta$-lg [approximately 90% pure (PAGE), 3× crystalllized and lyophilized; mixture of genetic variants A and B, reference L0103, Lot 095K7006] and HCl were obtained from Sigma-Aldrich (Ireland). WPI BioPro [~98% (w/w) protein on a dry basis: 65% $\beta$-lg, 25% α-lactalbumin, and 8% bovine serum albumin] was obtained from Davisco Foods International, Inc. (Le Sueur, MN). Phosphotungstic acid was purchased from Agar Scientific (Stansted, Essex, U.K.). Molecular-weight standards were purchased from GE Healthcare (Chalfont, St. Giles, U.K.). Purified water [Milli-Q water, resistivity (18.2 MΩ cm, at 25 °C), Millipak Express] was used throughout. All other reagents were analytical-grade.

**Protein Dispersions.** A total of 2 g of $\beta$-lg or WPI was dispersed in 98 g of Milli-Q water and stirred overnight to ensure full hydration of the protein, and the pH was adjusted to 2.0 using 6 M HCl. Dispersions were centrifuged at 45000*g* for 3 h at 25 °C. The supernatant was filtered through 0.45 $\mu$m low-protein filters (Minisart, Sartorius, Germany) and, subsequently, heated at 80 °C in a water bath (Grant, JPAT, Ltd.).

**AC-Mode AFM.** $\beta$-lg dispersions were investigated using a MFP-3D atomic force microscope (Asylum Research UK, Ltd., Oxford, U.K.). Samples of $\beta$-lg heated at 80 °C for 0 min, 15 min, 35 min, 45 min, 65 min, 85 min, 100 min, 200 min, 300 min, and 20 h, respectively, were used for AFM analysis. Prior to imaging, the dispersions were diluted in Milli-Q water to a final concentration of 20 g $L^{-1}$ (pH 2.6 ± 0.3) to facilitate imaging of single fibrils. Selected samples were also diluted in HCl (pH 2.0) for AFM imaging to confirm whether dilution affected the fibril appearance. No differences were observed between images obtained after water or HCl dilution, and to simplify the paper, only images obtained from water-diluted solutions are presented. Thus, 10 $\mu$L of $\beta$-lg diluted with Milli-Q water was deposited onto a freshly cleaved mica surface and subsequently dried in a desiccator. An aluminum reflex coating cantilever with a tetrahedral tip (AC 240; spring constant, 1.8 N/m; resonant frequency, 79.58 kHz; Olympus Optical Co., Ltd., Japan) and scan rate at 1 Hz was used for air-dried samples. The tetrahedral shape is ideal for obtaining precise morphology of soft samples because of its high lateral resolution. The radius of curvature of the tetrahedral tip was less than 10 nm. For imaging in water, $\beta$-lg or WPI dispersions were diluted in Milli-Q water as described above. A total of 100 $\mu$L of diluted $\beta$-lg was deposited on the mica surface. After a period of 10 min to allow for protein adsorption, AFM images were obtained using sharp and tall V-shaped "Biolever 150" silicon nitride tips (spring constant, 0.03 N/m; Olympus Optical Co., Ltd., Japan). The radius of curvature of the tip was 40 ± 3 nm, with a tip height of 5 $\mu$m, which helped to prevent the cantilever from touching the specimen. Oscillatory frequencies in water were in the range of 5−7.5 kHz. The scan rate was set at 1 Hz. Mica was used as the substrate for all samples because of its flatness and overall negative charge when cleaved.

**STEM.** Samples of fibrillar dispersions were prepared for STEM using negative staining. A droplet of the $\beta$-lg sample, which had been diluted 1:10 in water, was deposited onto carbon support film on a 400 mesh copper grid (Agar Scientific, Ltd., Stansted, Essex, U.K.). Excess liquid was removed after 1 min, using filter paper. A drop of staining solution [0.1% (w/w) phosphotungstic acid] was added, and excess solution was removed after 30 s with filter paper. Electron micrographs were taken using a Zeiss Supra 40 VP field emission scanning electron microscope (Carl Zeiss, Cambridge, U.K.) fitted with a Gemini multimode STEM detector. Bright field STEM images were acquired at 20 kV.

**ATR−FTIR.** ATR−FTIR measurements of freshly prepared 2% (w/w) $\beta$-lg in water at pH 2 were performed using a Bruker Tensor 27 spectrometer (Bruker Optik, GmBH, Ettlingen, Germany) fitted with a thermally controlled BioATR Cell II, which was specifically designed for measuring proteins in aqueous solution. The spectra were acquired and averaged over 128 scans at a resolution of 4 $cm^{-1}$ using Bruker Opus 5.5 software. After atmospheric compensation for absorbance of $CO_2$ and $H_2O$ as vapor and solute, respectively, the amide I band (1600−1700 $cm^{-1}$) was vector-normalized and the spectrum of the unheated sample was subtracted from the spectra of heated samples. Spectra were obtained for native and heated $\beta$-lg. The samples were heated directly on the crystal of the BioATR Cell at 80 °C and measurements were performed at 1, 5, 10, 21, 29, 39, 48, 59, 73, 88, and 109 min corresponding to the early stages of fibril formation. Subsequent measurements were performed on samples heated in a water bath for 109 min, 134 min, 135 min, 140 min, 21 h, 22 h, and 26 h, transferred immediately onto the ATR microcell, sealed, and equilibrated at 80 °C for at least 5 min before measurement. This procedure was chosen to eliminate the effect of sample evaporation when samples were heated for long time periods (> 150 min) on the crystal.

**SDS−PAGE.** SDS−PAGE was performed according to the method of Laemmli (*22*) under reducing conditions. Sigma-grade $\beta$-lg was used for SDS−PAGE analysis. Native $\beta$-lg samples were placed in glass vials and heated at 80 °C in a water bath. The vials were removed from the bath at defined time intervals (0 min, 5 min, 10 min, 20 min, 30 min, 40 min, 100 min, and 20 h) and immediately cooled on ice. The heated and unheated $\beta$-lg samples were mixed with reducing sample buffer (62.2 mM Tris-HCl at pH 6.8, 20% glycerol, 2% SDS, and 5% $\beta$-merchaptoethanol) at a sample/buffer ratio of 1:14 and heated for 5 min at 90 °C. SDS−PAGE was performed using 12% polyacrylamide gels, at a constant voltage of 155 V in a Mini Protean II system (Bio-Rad, Alpha Technologies, Dublin, Ireland). The gels were stained with 0.5% Coomassie Brilliant Blue R-250 (Sigma-Aldrich, St. Louis, MO). Molecular-weight standards (~14.4, ~18, and 66 kDa) were run on the gel to allow for the estimation of the molecular weights of the samples.

## RESULTS AND DISCUSSION

**AFM of $\beta$-lg Fibrils.** To investigate the formation of $\beta$-lg fibrils, AFM height images were performed on $\beta$-lg dispersions [2% (w/w), pH 2] that were heated at 80 °C for 0 min, 15 min, 35 min, 45 min, 65 min, 85 min, 100 min, 200 min, 300 min, and 20 h, respectively. Changes of $\beta$-lg monomers into fibrils were monitored by AFM measurements in air (**Figure 1**). At pH 2, native $\beta$-lg appeared as a globular monomer with a height of approximately 2 nm (0 min in **Figure 1**). During heating for 1−45 min, the monomers swelled and deformed, forming aggregates (**Figure 1**). After 65 min of heating, monomers appeared to reduce in size. Upon prolonged heating (> 85 min), short and long paired fibrils with split ends were observed. The short fibrils were assumed to be precursors of the longer fibrils. At 100 min of heating, samples consisted of a mixture of small particles/aggregates and fibrils.

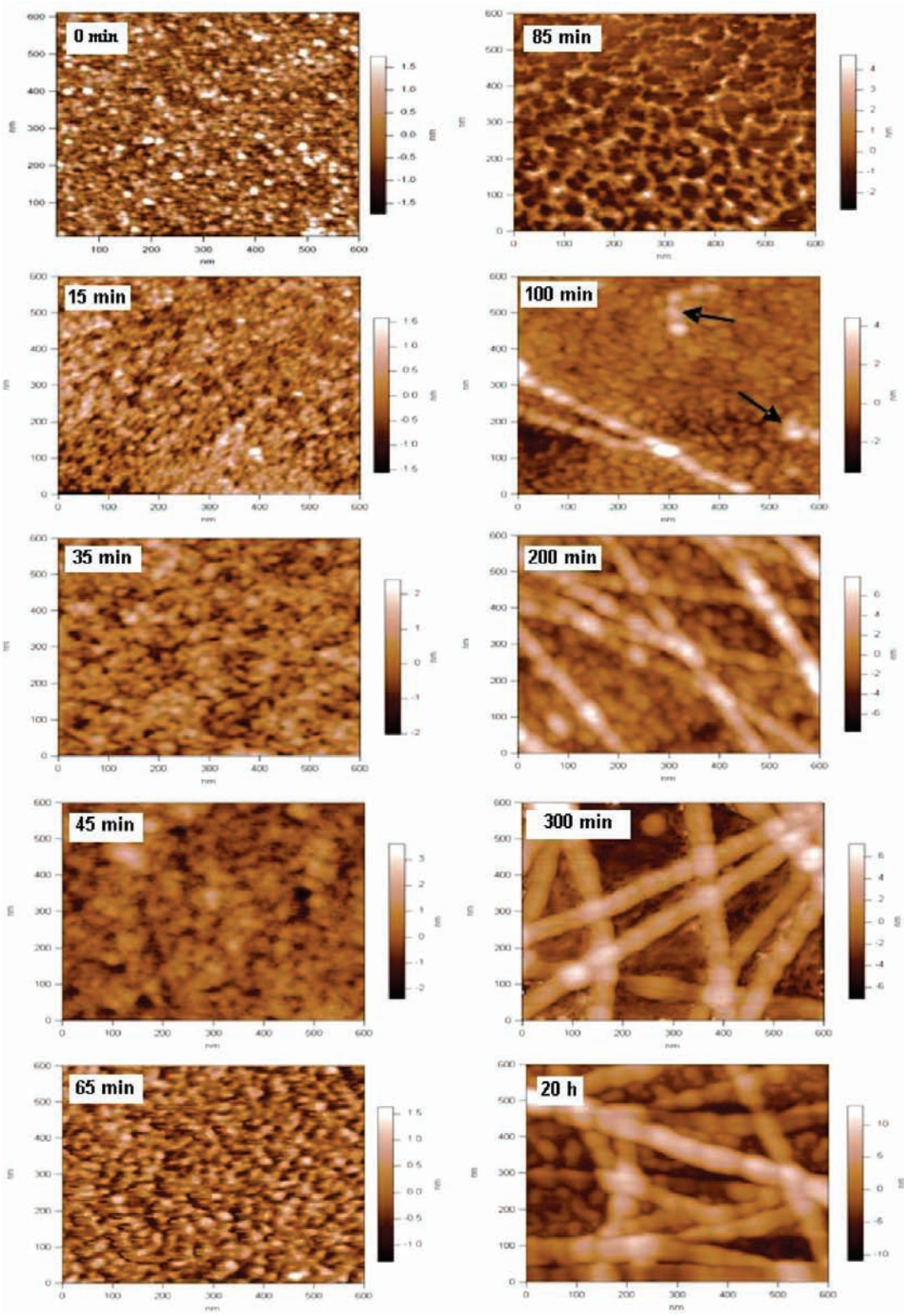


**Figure 1.** AFM height images of $\beta$-lg at pH 2 and 80 °C as a function of the heating time at 0 min, 15 min, 35 min, 45 min, 65 min, 85 min, 100 min, 200 min, 300 min, and 20 h. Images were obtained in air. Scan size = 600 nm. The arrows in the image at 100 min show the early stages of fibril formation.

Fibrillar subunits were observed after 200 min of heating (arrows in **Figure 2a**). More and longer fibrils were formed in samples heated from 300 min to 20 h (**Figure 3**). Single $\beta$-lg fibrils had a linear morphology and periodic structure, with a periodicity of ~30−40 nm (**Figure 2d**), heights of ~2−3 nm (**Figure 2c**), and lengths of up to 10 $\mu$m or more (**Figure 3a**). The thickness of overlapping fibrils was nearly 2 times higher (~6 nm) than single fibrils (panels **a** and **b** of **Figure 2**), with results being consistent with previous reports (*23*). The AFM phase image contrast provides high spatial resolution of surfaces, highlighting heterogeneities, and relative surface property differences, allowing for a clear distinction between fibril subunits (**Figure 2b**). Thus, it can be seen that subunits of well-developed fibrils exhibit similar mechanical properties (adhesion to the tip and hardness) because they induce the same changes in the phase image. Average fibril heights were calculated by measuring the tip height at various

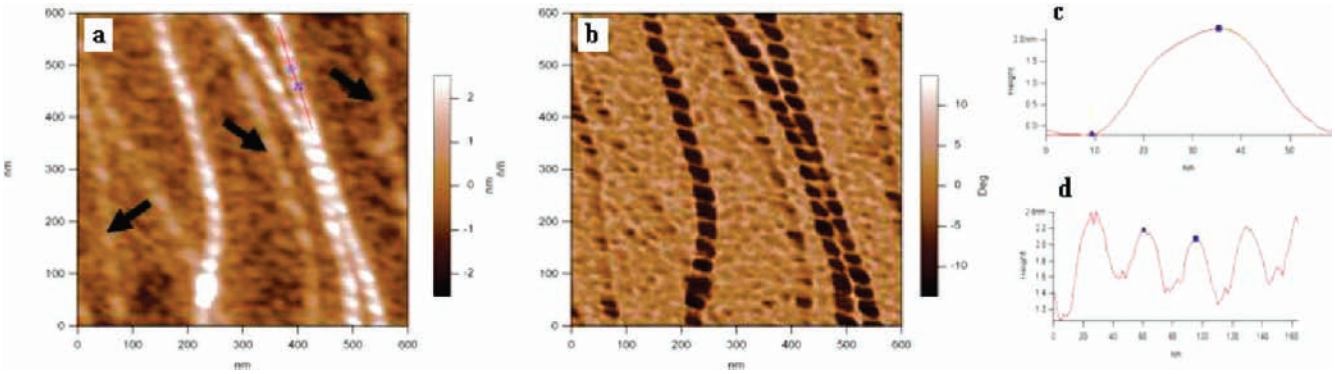


**Figure 2.** AFM (a) height and (b) phase images of $\beta$-lg at pH 2 and 80 °C heated for 200 min. $\beta$-lg fibrils had a (c) height of ~2−3 nm and a (d) periodicity of ~30 nm. Images were collected in air. Scan size = 600 nm. The arrows in the height image show the precursors of mature fibrils.

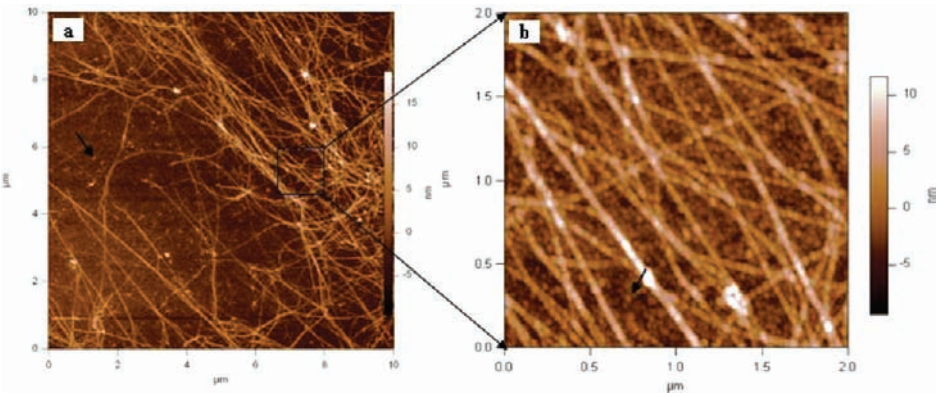


**Figure 3.** (a) 10 $\mu$m scan of AFM height images of $\beta$-lg at pH 2 and 80 °C heated for 20 h. Images were collected in air. The arrows indicate denaturated protein not incorporated into fibrils. (b) Magnified (2 $\mu$m scan) area of panel a, confirming the presence of non-incorporated proteins as well as fibrils.

points ($n$ = 10) for 10 different fibrils for each set of experiments. The cross-sectional height profiles, as measured using the MFP-3D software, demonstrate the periodicity of the fibrils and are shown in **Figure 2**. The results indicate that some denatured proteins are not incorporated into fibrils but form unordered aggregates, confirming the suggestion by Bolder et al. (*5*) that not all denatured and hydrolyzed $\beta$-lg is incorporated into fibrils even with prolonged heat treatment (they appear as white dots shown by the arrows in panels **a** and **b** of **Figure 3**). In this study, the height of the fibrils was smaller than those previously reported by Ikeda et al. (*6*), who studied $\beta$-lg dispersions at pH 2 in the presence of 0.1 M NaCl after heating at 80 °C. Ikeda and colleagues observed fibrils 4 nm in height, and they concluded that the fibrils consist of strings of partially unfolded $\beta$-lg monomers (*6*, *23*). AFM images of samples in water clearly show the $\beta$-lg fibrils and confirm their periodic nature (periodicity of 34 nm) (**Figure 4a**). Similar AFM experiments performed using WPI also showed the presence of fibrils. AFM height measurements in water show that WPI fibrils have similar characteristics to $\beta$-lg fibrils and occasionally showed paired fibrils in the form of a double helix with a periodicity of ~36 nm and height of ~7 nm (**Figure 4b**). The heights of single fibrils imaged in water ranged between 2.9 and 4.3 nm. Fibrils with periodic structures were seen in both the air and the water (height) images, demonstrating that the periodicity and dimensions are real and not an artifact because of air drying. However, small differences between height values measured in the two modes can be observed; these are inevitable because in air the fibril volume will decrease upon drying. Measurements in air using AFM indicated a loss in height of ~25% compared to the values obtained for measurements in liquid. These observations were in agreement with Moreno-Herrero et al. (*24*), who studied Alzheimer paired helical filaments imaged under physiological conditions and in air environments using AFM.

**STEM of $\beta$-lg Fibrils.** Electron microscopy confirmed the presence of fibrils, indicating that these features were not caused by the charged mica surface, as assumed previously (*19*) (**Figure 5**). The diameters of fibrils, measured from STEM images using the microscope software, were approximately 3 nm, which is comparable to the heights measured by AFM.

**ATR−FTIR of $\beta$-lg Fibrils Formation.** ATR−FTIR experiments allowed *in situ* observation of changes in the secondary structure during the denaturation and self-assembly processes of $\beta$-lg at 80 °C. The amide I band (1600−1700 $cm^{-1}$) of ATR−FTIR spectra is very sensitive to changes in the secondary structure of $\beta$-lg during the denaturation and aggregation processes (*25*, *26*). The spectra of native and heated $\beta$-lg (**Figure 6**) illustrate that heat treatment at pH 2 had a pronounced effect on the secondary structure of the protein. Curve fitting of the amide I band of $\beta$-lg incubated at pH 2.0 and heated for 1 min at 80 °C revealed absorption bands at 1614, 1624, 1631, 1640, 1650, 1660, 1670, and 1680 $cm^{-1}$, which are in good agreement with those in the literature (*21*, *25*, *26*). The observed amide I band is a complex composite, consisting of a number of overlapping component bands representing α helices (1654 $cm^{-1}$), low- and high-frequency components of $\beta$ structures (1630 and 1670 $cm^{-1}$), turns (1681 $cm^{-1}$), and random coils (1645 $cm^{-1}$), corresponding to the disordered parts of polypeptide backbones (*27*). During heating, hydrogen bonds stabilizing the native structure of $\beta$-lg are disrupted, causing the loss of α helices and $\beta$ sheets, and new intermolecular antiparallel $\beta$ sheets can be created (panels **a** and **b** of **Figure 6**).

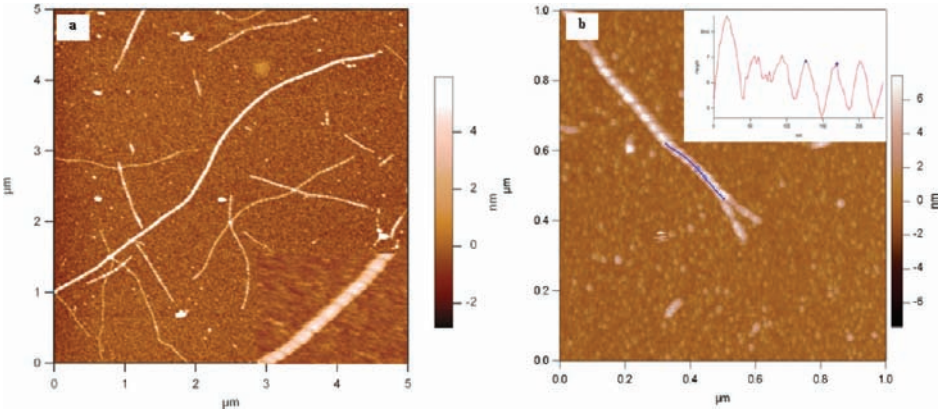


**Figure 4.** (a) AFM height image of $\beta$-lg at pH 2 and 80 °C heated for 20 h and imaged in water (pH 2.6). Fibril height values were 3 nm. (Inset) Higher resolution height image of 1 × 1 $\mu$m area, confirming periodicity of fibrils. (b) AFM height image of WPI fibrils at pH 2 and 80 °C heated for 20 h and imaged in water. (Inset) Cross-section height profile along the fibril axis highlighting periodicity.

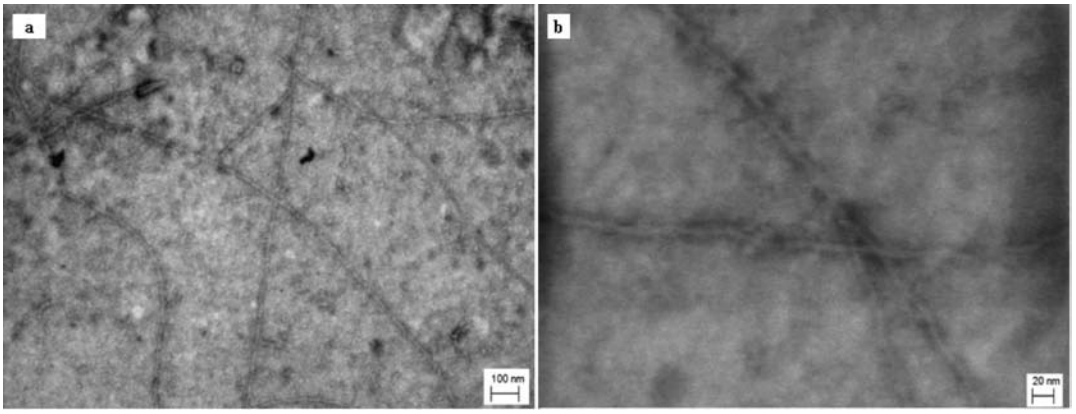


**Figure 5.** STEM negatively stained image of 2.0% (w/w) $\beta$-lg at pH 2 and 80 °C heated for 20 h. Scale bar = (a) 100 nm and (b) 20 nm.

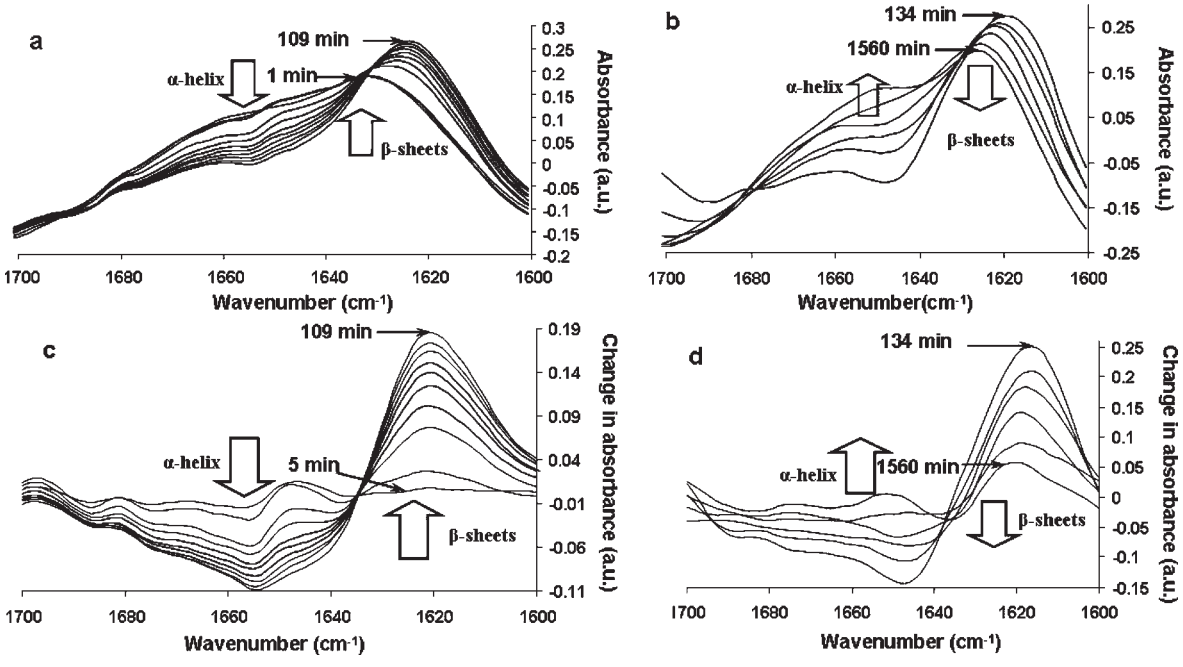


**Figure 6.** Amide I ATR−FTIR spectra of 2% (w/w) $\beta$-lg heated at 80 °C varying (a) from 1 to 109 min and (b) from 134 min to 26 h. Amide I spectra of the heated samples after native $\beta$-lg spectrum subtraction varying (c) from 5 to 109 min and (d) from 134 min to 26 h.

The increase in intensity of a specific band (1624 $cm^{-1}$) was attributed to the formation of extensive regions of $\beta$ sheets involved in intermolecular cross-linking between unfolded proteins and characterized protein aggregation (*18*, *28*−*32*). Subtraction of the native spectra from those of the heated sample showed that there was a significant increase in the absorbance at

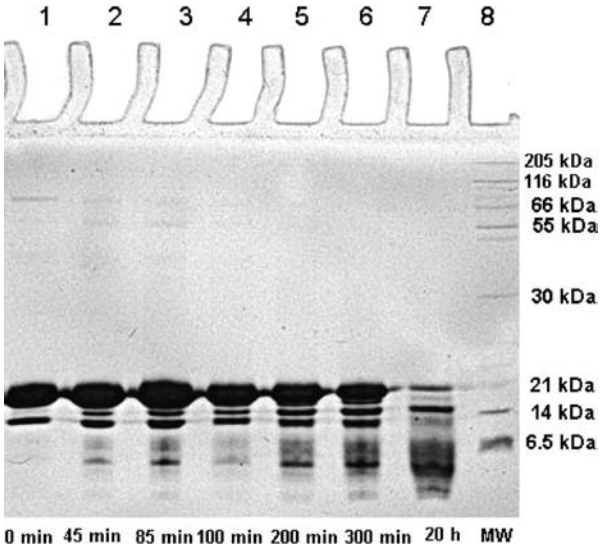


**Figure 7.** SDS−PAGE of 2% (w/w) $\beta$-lg at pH 2, heated at 80 °C for various heating times. Lane 8, polypeptide molecular-weight marker (~14.4 kDa for α-lactalbumin, ~18.4 kDa for $\beta$-lg, and ~67 kDa for bovine serum albumin). Lanes 1−7 represent $\beta$-lg heated for 0 min, 45 min, 85 min, 100 min, 200 min, 300 min, and 20 h, respectively.

1624 $cm^{-1}$ (panels **c** and **d** of **Figure 6**). The bands at 1646, 1630, and 1624 $cm^{-1}$ broaden, suggesting a general loss in secondary structure.

The ATR−FTIR results suggest that the fibril formation process takes place in two stages. In the first stage (up to approximately 100 min heating time), a decrease in the α-helical content and an increase in intermolecular $\beta$-sheet content were observed, similar to those associated with disordered aggregates (*21*). The second stage (between 100 min and 26 h) is accompanied by a decrease in $\beta$-sheet content and a slight increase in α-helical content, corresponding to the formation long fibrils after prolonged heating. Changes in the secondary structures are due to protein degradation, fibril assembly, and protein reorganization in the fibril. When the AFM results are taken into account, in the first stage, the $\beta$-lg proteins denature, become partially unfolded, and gradually degrade. All of these phenomena lead to an increase in the amount of $\beta$-sheet content. In the second stage, the decreased amount of $\beta$-sheet content is associated with the formation of long fibrils.

**SDS−PAGE.** Reducing SDS−PAGE results showed that native $\beta$-lg monomers have a broad band around 18.4 kDa (0 min, lane 2 in **Figure 7**). No significant changes were observed for heating times shorter than 45 min. Above a heating time of 45 min, protein fragments (peptides) smaller than the $\beta$-lg monomers were detected (lanes 3−7 in **Figure 7**). It can be seen from the AFM results (**Figure 1**) that $\beta$-lg dispersions heated for 100 min contain a mixture of aggregates and short fibrillar structures. Thus, the low-molecular-weight protein fragments observed during SDS−PAGE experiments indicate that these assemblies could be broken down by the reducing sample buffer. It has recently been shown that $\beta$-lg at pH 2, heated at 80 °C (from 25 min to 24 h), is hydrolyzed into peptides (*14*). AFM and STEM results show that only the dispersions heated for > 300 min contain very long fibrils (> 10 $\mu$m), together with some nonfibrillar protein particles, which were not incorporated into fibrils. In lane 7, only peptides were observed, suggesting that $\beta$-lg fibrils were composed of peptide fragments. These observations appear to contradict previous studies that indicate that protein fibrils are not completely broken down by SDS-reducing buffers (*5*, *14*). This may be attributed to lower protein concentrations and higher buffer concentrations used when heating the sample in reducing sample buffer. It should also be noted that no stained proteinaceous material was seen either at the top of the stacking gel or within the wells. Furthermore, no fibrillar material was detected by AFM or SEM analysis of fibril dispersions prepared in SDS-reducing buffer under our experimental conditions (results not shown), suggesting that fibrils had been dissociated. These observations indicate that the effect of chaotropic agents on protein fibrils is complex and warrants further systematic study. It can therefore be tentatively concluded that $\beta$-lg components within the nanofibrils were associated via non-covalent interactions (*5*). This fibril formation mechanism contrasts with that of fibrils formed at higher ionic strength, which is characterized by shorter fibrils formed from partially intact $\beta$-lg monomers or dimers (*23*).

## CONCLUSIONS

Studies using AFM, STEM, real-time ATR−FTIR, and SDS−PAGE were performed to investigate the fibrillar aggregation process of $\beta$-lg. This study demonstrates that AFM imaging combined with more established analytical techniques gives unique insight into the transformation of native proteins into fibrillar structures. The sequence of AFM images of $\beta$-lg dispersions clearly demonstrates the progress of fibril aggregation as a function of the heating time. STEM results confirm AFM observations of $\beta$-lg fibrils in air and in water. This study shows, for the first time, AFM imaging of $\beta$-lg and WPI-derived fibrils in water under ambient conditions and the presence of double-helical structures *in situ*. SDS−PAGE analysis suggests that $\beta$-lg fibrils consist of polypeptide fragments linked via non-covalent intermolecular bonds and are not formed from intact monomers. The real-time monitoring of the assembly processes *in situ* using ATR−FTIR correlated with AFM and SDS−PAGE results, suggesting a two-stage mechanism of fibril formation: (1) denaturation, partial unfolding, and increase in $\beta$-sheet content with hydrolysis of monomers followed by (2) linear aggregation of polypeptide fragments into fibrils via non-covalent interactions, continued hydrolysis, and an accompanying decrease in $\beta$-sheet content and overall secondary structure.

## ACKNOWLEDGMENT

The authors thank Amir Moshar (Applications Scientist, Asylum Research, U.K.) for his assistance with AFM imaging in liquids.

## LITERATURE CITED

(1) Bolder, S. G.; Hendrickx, H.; Sagis, L. M. C.; van der Linden, E. Fibril assemblies in aqueous whey protein mixtures. *J. Agric. Food Chem.* **2006**, *54*, 4229–4234.

(2) Rogers, S. S.; Venema, P.; Sagis, L. M. C.; van der Linden, E.; Donald, A. M. Measuring length distribution of a fibril system: A flow birefringence technique applied to amyloid fibrils. *Macromolecules* **2005**, *38*, 2948–2958.

(3) Qi, X. L.; Holt, C.; McNulty, D.; Clarke, D. T.; Brownlow, S.; Jones, G. R. Effect of temperature on the secondary structure of $\beta$-lactoglobulin at pH 6.7, as determined by CD and IR spectroscopy: A test of the molten globule hypothesis. *Biochem. J.* **1997**, *324*, 341–346.

(4) Aymard, P.; Nicolai, T.; Durand, D.; Clark, A. Static and dynamic scattering of $\beta$-lactoglobulin aggregates formed after heat-induced denaturation at pH 2. *Macromolecules* **1999**, *32*, 2542–2552.

(5) Bolder, S. G. V.; Sagis, A. J.; Leonard, M. C.; van der Linden, E. Heat-induced whey protein isolates fibrils: Conversion, hydrolysis, and disulphide bond formation. *Int. Dairy J.* **2007**, *17*, 846–853.

(6) Ikeda, S.; Morris, V. J. Fine-stranded and particulate aggregates of heat-denatured whey proteins visualized by atomic force microscopy. *Biomacromolecules* **2002**, *3*, 382–389.
(7) Arnaudov, L. N.; de Vries, R.; Ippel, H.; van Mierlo, C. P. M. Multiple steps during the formation of β-lactoglobulin fibrils. *Biomacromolecules* **2003**, *4*, 1614–1622.
(8) Akkermans, C.; van der Goot, A. J.; Venema, P.; Gruppen, H.; Vereijken, J. M.; van der Linden, E.; Boom, R. M. Micrometer-sized fibrillar protein aggregates from soy glycinin and soy protein isolate. *J. Agric. Food Chem.* **2007**, *55*, 9877–9882.
(9) Mounsey, J. S.; O'Kennedy, B. T.; Fenelon, M. A.; Brodkorb, A. The effect of heating on β-lactoglobulin−chitosan mixtures as influenced by pH and ionic strength. *Food Hydrocolloids* **2008**, *22*, 65–73.
(10) Weiss, J.; Takhistov, P.; McClements, J. Functional materials in food nanotechnology. *J. Food Sci.* **2006**, *71*, R107–R116.
(11) Arnaudov, L. N.; de Vries, R. Critical concentration for fibrillar aggregation of bovine β-lactoglobulin. *Food Colloids: Interactions, Microstructure and Processing*; Dickinson, E., Ed.; Elsevier Science, Ltd.: Harrogate, U.K., 2005; Vol. 19, pp 237−246.
(12) Veerman, C.; Sagis, L. M. C.; Venema, P.; van der Linden, E. The effect of shear flow on the percolation concentration of fibrillar protein assemblies. *J. Rheol.* **2005**, *49*, 355–368.
(13) Ikeda, S. Atomic force microscopy and Raman scattering spectroscopy studies on heat-induced fibrous aggregates of β-lactoglobulin. *Spectroscopy* **2003**, *17*, 195–202.
(14) Akkermans, C.; Venema, P.; van der Goot, A. J.; Gruppen, H.; Bakx, E. J.; Boom, R. M.; van der Linden, E. Peptides are building blocks of heat-induced fibrillar protein aggregates of β-lactoglobulin formed at pH 2. *Biomacromolecules* **2008**, *9*, 1474–1479.
(15) Morris, V. J.; Mackie, A. R.; Wilde, P. J.; Kirby, A. R.; Mills, E. C. N.; Gunning, A. P. Atomic force microscopy as a tool for interpreting the rheology of food biopolymers at the molecular level. *Food Sci. Technol.* **2001**, *34*, 3–10.
(16) Ortiz, C.; Zhang, D. M.; Ribbe, A. E.; Xie, Y.; Ben-Amotz, D. Analysis of insulin amyloid fibrils by Raman spectroscopy. *Biophys. Chem.* **2007**, *128*, 150–155.
(17) Vetri, V.; Canale, C.; Relini, A.; Librizzi, F.; Militello, V.; Gliozzi, A.; Leone, M. Amyloid fibrils formation and amorphous aggregation in concanavalin A. *Biophys. Chem.* **2007**, *125*, 184–190.
(18) Dahlgren, P. R.; Karymov, M. A.; Bankston, J.; Holden, T.; Thumfort, P.; Ingram, V. M.; Lyubchenko, Y. L. Atomic force microscopy analysis of the Huntington protein nanofibril formation. *Dis.-Mon.* **2005**, *51*, 374–385.
(19) Green, J. D.; Goldsbury, C.; Kistler, J.; Cooper, G. J. S.; Aebi, U. Human amylin oligomer growth and fibril elongation define two distinct phases in amyloid formation. *J. Biol. Chem.* **2004**, *279*, 12206–12212.
(20) Gosal, W. S.; Clark, A. H.; Ross, M. S. B. Fibrillar β-lactoglobulin gels: Part 1. Fibril formation and structure. *Biomacromolecules* **2004**, *5*, 2408–2419.
(21) Eissa, A. S.; Puhl, C.; Kadla, J. F.; Khan, S. A. Enzymatic cross-linking of β-lactoglobulin: Conformational properties using FTIR spectroscopy. *Biomacromolecules* **2006**, *7*, 1707.
(22) Laemmli, U. K. Cleavage of structural proteins during the assembly of the head of bacteriophage T4. *Nature* **1970**, *227*, 680–685.
(23) Ikeda, S. Heat-induced gelation of whey proteins observed by rheology, atomic force microscopy, and Raman scattering spectroscopy. *Food Hydrocolloids* **2003**, *17*, 399–406.
(24) Moreno-Herrero, F.; Perez, M.; Baro, A. M.; Avila, J. Characterization by atomic force microscopy of Alzheimer paired helical filaments under physiological conditions. *Biophys. J.* **2004**, *86*, 517–525.
(25) Allain, A. F.; Paquin, P.; Subirade, M. Relationships between conformation of β-lactoglobulin in solution and gel states as revealed by attenuated total reflection Fourier transform infrared spectroscopy. *Int. J. Biol. Macromol.* **1999**, *26*, 337–344.
(26) Lefevre, T.; Subirade, M. Molecular differences in the formation and structure of fine-stranded and particulate β-lactoglobulin gels. *Biopolymers* **2000**, *54*, 578–586.
(27) Kavanagh, G. M.; Clark, A. H.; Ross-Murphy, S. B. Heat-induced gelation of globular proteins: Part 3. Molecular studies on low pH β-lactoglobulin gels. *Int. J. Biol. Macromol.* **2000**, *28*, 41–50.
(28) Boye, J. I.; Ismail, A. A.; Alli, I. Effects of physicochemical factors on the secondary structure of β-lactoglobulin. *J. Dairy Res.* **1996**, *63*, 97–109.
(29) Bromley, E. H. C.; Krebs, M. R. H.; Donald, A. M. Aggregation across the length-scales in β-lactoglobulin. *Faraday Discuss.* **2005**, *128*, 13–27.
(30) Sawyer, L.; Kontopidis, G. The core lipocalin, bovine β-lactoglobulin. *Biochim. Biophys. Acta* **2000**, *1482*, 136–148.
(31) Croguennec, T.; Mollé, D.; Mehra, R.; Bouhallab, S. Spectroscopic characterization of heat-induced nonnative β-lactoglobulin monomers. *Protein Sci.* **2004**, *13*, 1340–1346.
(32) Guinand, S.; Tonnelat, J. Etude thermodynamique de la dissociation réversible de la β-lactoglobuline B pour des Ph supérieurs á 5.5. *Biochim. Biophys. Acta* **1962**, *59*, 737–739.

**Received for review August 11, 2009. Revised manuscript received February 15, 2010. Accepted February 15, 2010. This work was funded by the Irish Department of Agriculture and Food though the FIRM Project 06RDT-MFRC-432.**